

Institute of Electrical Engineering and Information Technology  
Paderborn University  
Department of Power Electronics and Electrical Drives  
Prof. Dr.-Ing. Joachim Böcker

**Master Project**

**Calorimetric Measuring Chamber  
Optimization**

by

Vijay Kumar Reddy Thera, Syed Sarim Zuhair Haider

Student ID: 6944080, 6988465

Supervisor: Daniel Urbaneck, Nikolas Förster

Filing Date: October 17, 2023

---

# Abstract

---

The Calorimetric Measuring Chamber serves as the means for calculating the power losses of the Device Under Test (DUT) located within the test chamber. The primary aim of this project is to optimize the calorimetric measuring chamber by designing a system capable of accurately controlling the temperature of the inlet water to the inner heat exchanger, maintaining a stable, predefined temperature within the inner chamber.

This system utilizes a cooler to prevent unnecessary fluctuations in water temperature caused by changes in ambient temperature, and a heater to rapidly heat up the inner chamber to a specific set temperature. The cooler and heater are powered by buck and buck-boost converters, respectively, situated on the calorimeter power module Printed Circuit Board (PCB). Temperature regulation within the inner chamber is achieved by adjusting the power supplied to the heater, while the cooler's power is controlled to regulate the temperature of the inlet water.

To accomplish this, a cascaded control system with a temperature controller and voltage controller is implemented to ensure precise temperature regulation. The temperature controller relies on temperature sensor data provided by the Calorimeter mainboard. To facilitate data exchange, Serial Peripheral Interface (SPI) communication is established between the Calorimeter mainboard and the power module. The project includes conducting power loss measurement tests on multiple DUTs at different set temperatures and redesigning the power module PCB to enhance its functionality. Ultimately, the project aims to deliver an optimized system capable of maintaining precise temperature control throughout the testing process.

---

# Contents

---

<b>1</b>	<b>Introduction</b>	<b>1</b>
1.1	System description . . . . .	1
1.2	Objectives . . . . .	3
1.3	Task Description . . . . .	4
<b>2</b>	<b>Controller design</b>	<b>5</b>
2.1	Introduction . . . . .	5
2.2	Purpose . . . . .	5
2.3	Transfer Function Analysis . . . . .	6
2.4	Controller Selection . . . . .	7
2.4.1	Frequency Analysis . . . . .	7
2.5	Programming and Testing . . . . .	10
2.5.1	Application on Micro-controller . . . . .	10
<b>3</b>	<b>SPI communication</b>	<b>11</b>
3.1	Protocol . . . . .	11
3.2	Implementation and Testing . . . . .	12
<b>4</b>	<b>Initial tests with heater and cooler - Milestone</b>	<b>13</b>
4.1	Observations . . . . .	13
<b>5</b>	<b>Trip-zone implementation</b>	<b>14</b>
<b>6</b>	<b>Power module PCB new version</b>	<b>15</b>
6.1	Testing . . . . .	16
<b>7</b>	<b>GUI updates</b>	<b>17</b>
7.1	Purpose . . . . .	17
7.2	Updates . . . . .	17
7.3	Integration and Testing . . . . .	19
<b>8</b>	<b>Cascaded control</b>	<b>20</b>
8.1	Overview . . . . .	20
<b>9</b>	<b>Final tests and results</b>	<b>22</b>

<b>10 Conclusion and Future work</b>	<b>25</b>
10.1 Future Work . . . . .	25
<b>Appendix</b>	<b>26</b>
A.1 GUI . . . . .	26
A.2 CCS program . . . . .	26
<b>Lists</b>	<b>27</b>
List of Tables . . . . .	27
List of Figures . . . . .	27
Acronyms . . . . .	27
Glossary . . . . .	27
Nomenclature . . . . .	28
References . . . . .	28

---

# 1 Introduction

---

Measuring power losses by comparing the input and output power is now accurate enough for DC-DC converter systems. However, in AC systems, particularly those with harmonics, phase errors and electrical noise is challenging. An alternative approach is to measure the direct heat losses that happen in the power system, and this is known as the calorimetric method. Especially in the context of flow calorimetry, all the heat generated by the Device Under Test (DUT) is collected by a coolant, like water, as it flows through the heat exchanger. The power loss of DUT is calculated using the formula 1.1, by measuring the flow rate and temperature change of water while it circulates through the Heat exchanger [1].

$$P_{calculated} = c \cdot \dot{V} \cdot \rho \cdot (T_{in} - T_{out}) \quad (1.1)$$

with  $c$  the specific heat of the water, the flow rate  $\dot{V}$  of the water, the mass density  $\rho$  and the difference between  $T_{in}$  inlet water temperature and  $T_{out}$  outlet water temperature.

## 1.1 System description

In the past years, a closed double-cased type calorimeter was designed and developed at Paderborn University. Fig. 1.1 shows the developed calorimetric measuring chamber. The target specification is the determination of power losses up to 600 W. The closed double-cased type calorimeter allows active control of the air temperature in the gap  $T_{gap}$  between the inner and outer chamber with the help of heating foils and thereby prevents heat leakage through the walls. This system allows us to compute the power losses of the DUT within the test chamber.

However, a significant issue is that it takes more than 8 hours to obtain accurate power loss calculations. This extended time frame is primarily because the heat generated by the DUT, representing power loss, not only transfers to the coolant but also warms the entire inner chamber to a uniform temperature. Additionally, another problem arises from fluctuations in the inlet water temperature  $T_{in}$ , this temperature change will directly affect the calculated power loss. This variation is a consequence of the fact that the water exiting the inner heat exchanger absorbs heat from the inner chamber, causing it to become hot. Subsequently, the water is cooled down to the ambient temperature using an air-cooled outer heat exchanger before circulating back to the inner heat exchanger.

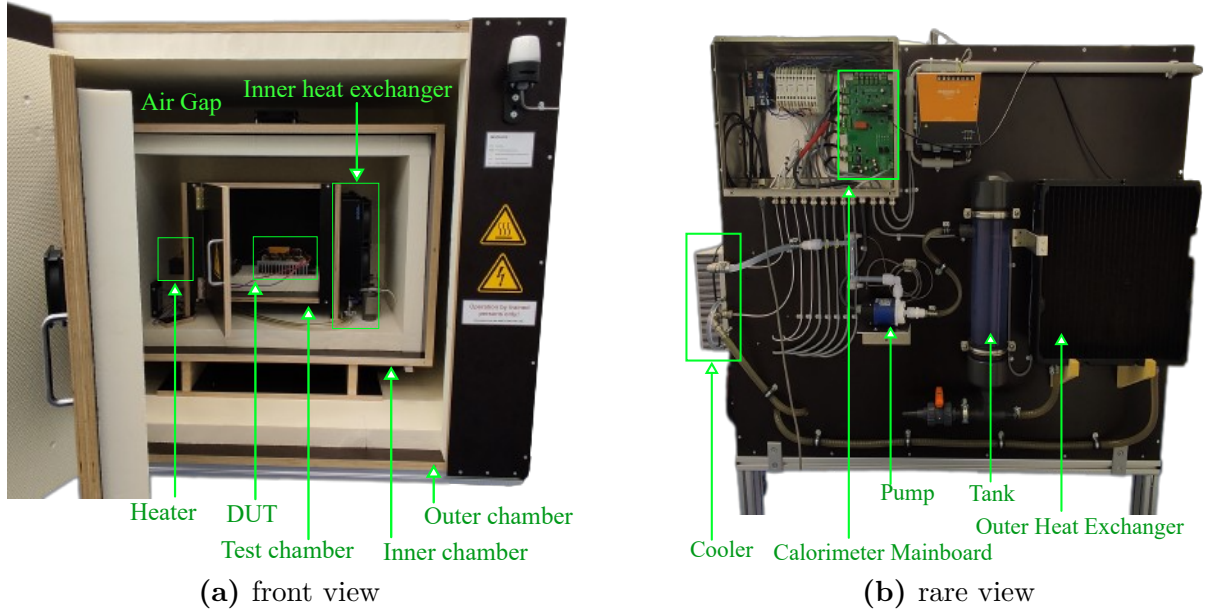


**Fig. 1.1:** Closed double-cased type calorimetric measuring chamber

These two problems are solved by adding controlled heating and cooling systems respectively. To speed up the process of warming the inner chamber, the heating system is put to use. The heating system consists of a controlled DC power supply, temperature controller, and 100 W heating resistor referred to as a heater. Its role is to generate heat, thus accelerating the warming of the inner chamber to the user-defined temperature, while also maintaining this temperature consistently during power loss calculation. To mitigate fluctuations in the water temperature caused by changes in the surrounding environment, a cooling system is introduced. The cooling system is composed of a controlled DC power supply, a temperature controller, and a 200 W Peltier cooler, referred to as a cooler. Its role is to cool the water down to a user-defined temperature and uphold a stable water inlet temperature  $T_{in}$ .

The concept of integrating heating and cooling systems into the calorimeter was examined by employing two separate programmable power supplies, along with a PC that ran a temperature control program via MATLAB [2]. This setup aimed to manage power for both the cooler and heater. Although this approach demonstrated effectiveness, it ultimately revealed itself to be excessively complex and not suitable for practical use. Additionally, the power supplies were excessively over-dimensional for a 300 W system. This raises the necessity for designing and developing a calorimeter power module system. This comprises a power module PCB [3], which features a buck converter for powering the cooler and a buck-boost converter for powering the heater. Additionally, a microcontroller is responsible for temperature regulation, and a debugger aids in system troubleshooting. The power module PCB is additionally equipped with voltage and current measurement circuits for measuring the output voltages and currents of both converters. These measurements will

be valuable for voltage control and also in the computation of output power. In the past, the power module PCB was developed and subjected to testing using an electronic load, reaching up to 200 W for both converters, while operating in an open-loop configuration. The fig.1.2 represents the optimized calorimetric measuring chamber after integrating the power module, cooling, and heating systems. The inner chamber after optimizing comprises the heater, DUT, and fans. Fans aid in evenly distributing heat throughout the inner chamber. The calculated heat loss now encompasses the power loss of the heater, the fan power loss, and the DUT loss. To determine the DUT loss, we can straightforwardly deduct the heater power and fan power losses from the total calculated power.

$$P_{DUT} = P_{calculated} - P_{heater} - P_{fan} \quad (1.2)$$

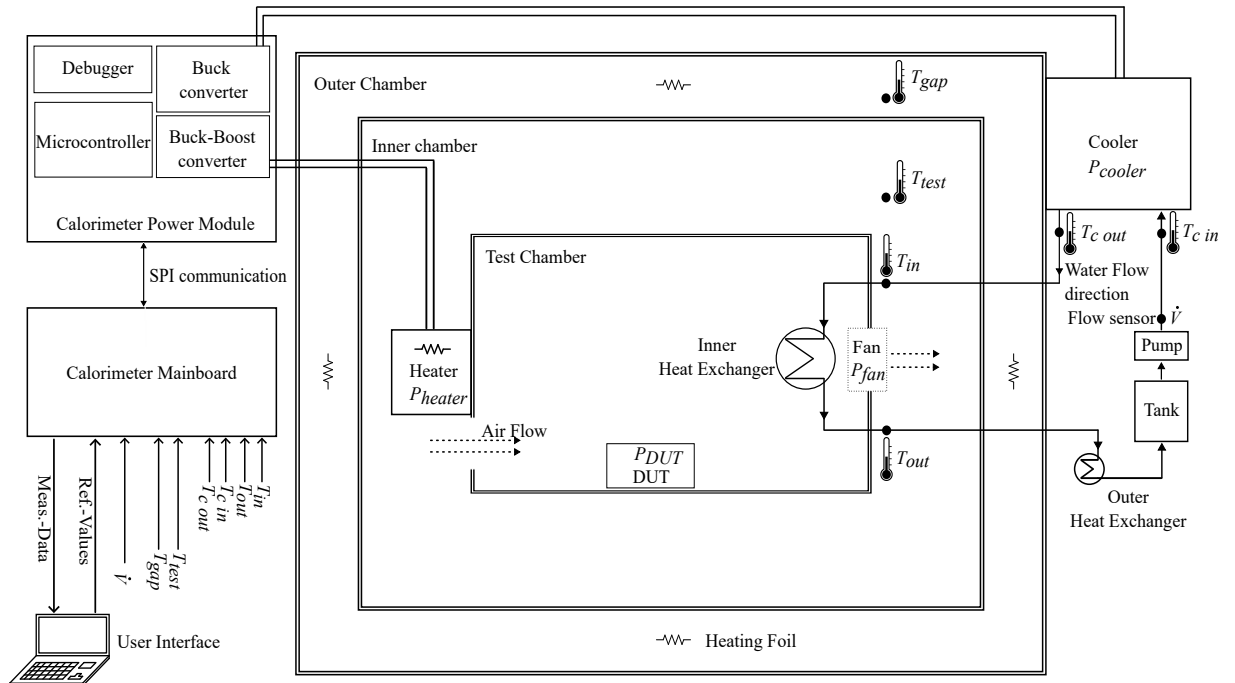


**Fig. 1.2:** Schematic representation of optimized calorimetric measuring chamber

## 1.2 Objectives

The main objective of this project is to integrate the power module system with the calorimeter chamber, enabling precise control of both the water inlet temperature  $T_{in}$  and the temperature within the inner chamber  $T_{test}$ . Achieving this aim necessitates establishing communication between the microcontroller on the calorimeter mainboard and the microcontroller on the power module. This communication facilitates the exchange of temperature data and user-defined values, allowing the power module to regulate the heater and cooler power, thereby ensuring precise temperature control within the system. An integral part of this project involves developing a cascaded control system, a crucial

step in achieving optimal system performance. Additionally, it involves thorough testing of the optimized system, including the measurement of power losses for various DUTs across a range of user-defined values.

### 1.3 Task Description

The approach to achieving project goals involves the following fundamental steps:

- Cascaded controller design and implementation: The first step is to design and implement a cascaded control system that encompasses both an outer temperature controller and an inner voltage controller. This control system will ensure precise and responsive temperature regulation for all system components.
- SPI communication implementation: To establish communication between the calorimeter mainboard and the power module, implementing the Serial Peripheral Interface (SPI) communication. This communication is essential for data exchange and coordination between these critical components.
- Power module redesign: Redesigning the power module to accommodate all modifications, corrections, and updates. This step ensures the optimal functionality of the Power Module PCB.
- Testing across multiple operation points: This stage encompasses a comprehensive testing process for the optimized system, which includes calculating power losses for different DUTs under a variety of user-specified parameters.



---

## 2 Controller design

---

### 2.1 Introduction

In the realm of electrical engineering and circuit design, it is a well-established fact that voltage supply deviations and voltage drops across various components within a circuit are intrinsic phenomena. While these voltage variations are not typically accounted for in the idealized framework, the practical reality of working with real-world, non-ideal circuits necessitates a thorough consideration of these losses and inherent behaviors to effect appropriate remedies.

### 2.2 Purpose

To mitigate and address such voltage losses and disruptions, the discipline of control design assumes a pivotal role. Control design manifests in various manifestations, encompassing pole-zero plots or frequency response plots, both relevant to analog and digital systems. Within this context, control design serves as the blueprint that comprehensively defines the circuit's characteristics and governs its overall behavior, determining whether it operates in a stable or unstable manner.

Through a meticulous analysis of the circuit and the strategic introduction of requisite poles or zeros into the system, control design imparts robustness. This robustness, in turn, equips the system with the capacity to adapt to voltage losses and disruptions, ultimately facilitating the delivery of the desired output.

In the case of system under consideration, following is a block diagram depiction of the controller with the converters and the test chamber.

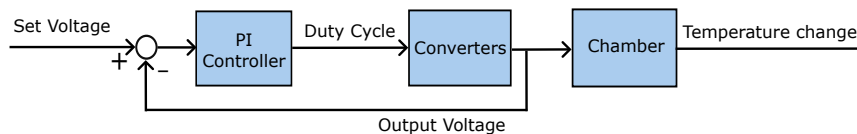


**Fig. 2.1:** Inner Control Loop

## 2.3 Transfer Function Analysis

In the context of converter systems, whether they take the form of a Buck converter or a Buck-Boost converter, it becomes imperative to undertake a comprehensive investigation of their transfer functions.

In the system under consideration, power supplied to the heater and cooler is being controlled by means of the voltage. Therefore, for a power requirement of 0 to 200 Watts it is essential to use a converter that can boost and step down the voltage level simultaneously according to the need of the system. Hence, for this use case a Buck-Boost converter is used which acts as a power supply for the heating element in the system. In addition to that, the power rating required for the cooler is in the range of 0 to 100 Watts which can easily be satisfied by using a Buck converter. Therefore, a Buck converter is used as a power supply for the cooler.

In this context, the transfer functions with the design aspects, corresponding to these specific converters are mathematically articulated as follows.

For Buck-Boost converter:

$$TF_{Buck-Boost} = \frac{v_o}{D} = \frac{(V_g + V_o) - \frac{Ls+R_L}{D_2} I_L}{D_2(s^2(\frac{LC}{D_2^2}) + s(\frac{R_L C + \frac{L}{R}}{D_2^2}) + (1 + \frac{R_L}{D_2^2}))} \quad (2.1)$$

Design aspects for Buck-Boost Converter		
Quantities	Symbol	Values
Resistance	$R$	$6\Omega$
Inductance	$L$	$65\mu\text{H}$
Capacitance	$C$	$880 \mu\text{F}$
Input Voltage	$V_g$	$24\text{V}$
Parasitic R	$R_L$	$6.2\text{m}\Omega$
Set Voltage	$V_o$	$10.96\text{V}$
Off Duty Cycle	$D_2$	$0.69$

For Buck Converter:

$$TF_{Buck} = \frac{v_o}{D} = \frac{V_g}{s^2(LC) + s((R_L C) + (\frac{L}{R})) + (1 + (\frac{R_L}{R}))} \quad (2.2)$$

Design aspects for Buck Converter		
Quantities	Symbol	Values
Resistance	$R$	$2.33\Omega$
Inductance	$L$	$65\mu\text{H}$
Capacitance	$C$	$660\mu\text{F}$
Input Voltage	$V_g$	$24\text{V}$
Parasitic R	$R_L$	$6.2\text{m}\Omega$

The crux of this analysis predominantly unfolds within the frequency domain, affording us the capability to gain insights into the operational characteristics of these converters across a broader spectrum of frequencies.

## 2.4 Controller Selection

In the realm of control systems, selecting an appropriate control methodology is contingent upon a meticulous analysis of the frequency response characterizing the respective systems under consideration.

### 2.4.1 Frequency Analysis

In the realm of converter systems, the imperative need for frequency analysis arises from the intrinsic characteristics that distinguish these systems from conventional linear time-invariant systems. Converter systems are characterized by their propensity to exhibit intricate frequency-dependent behaviors, an attribute stemming from the complex interplay of multiple elements within the system. These elements encompass the switching dynamics, the presence of filtering components, and the intricacies of control system design. Consequently, a departure from conventional methods of analysis, which often center on the time-domain representation, becomes necessary.

Crucially, the frequency-dependent behavior observed in converter systems necessitates a thorough examination of the system's characteristics in the frequency domain, an endeavor that can be effectively accomplished through the construction and scrutiny of Bode plots. In this context, the Bode plots serve as an indispensable analytical tool, yielding invaluable insights into the system's frequency response, gain, and phase characteristics as a function of frequency variation. The gain and phase margins, as gleaned from the Bode plots, emerge as pivotal metrics that underpin the stability and robustness of the system. These margins assume the role of critical benchmarks, determining the system's capacity to remain stable in the face of perturbations and disturbances. Moreover, they provide essential guidance for engineers and control system designers in their quest to craft converter systems that fulfill stringent performance criteria and offer the requisite resilience in the presence of unpredictable external factors.

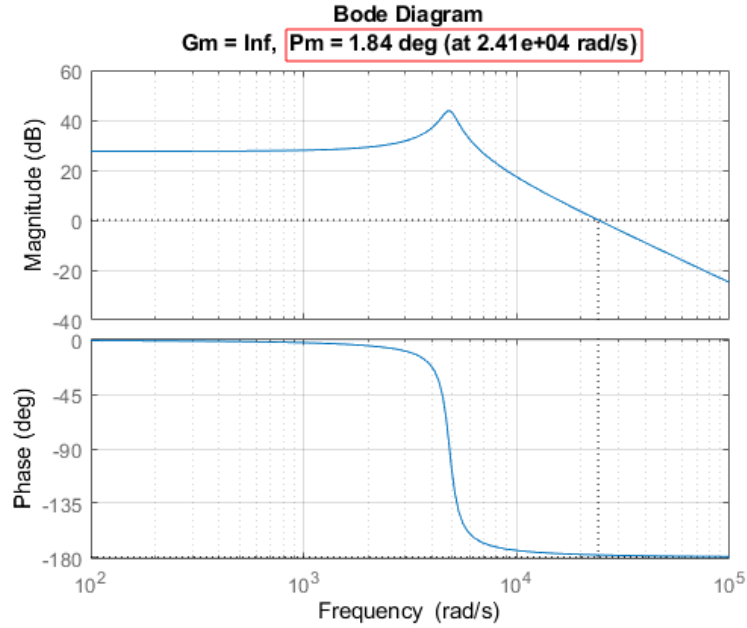


**Fig. 2.2:** Uncompensated Frequency Response of Buck Converter

#### 2.4.1.1 Buck Converter

The Bode plot in fig. 2.2 of the buck converter under consideration in equation 2.2 (from [4]) depicts a nearly stable system from the phase margin but the response exhibits a steady state error. Therefore, the system requires a low-frequency pole or a lag compensator. However, it is essential to consider that a lag compensator alone reduces the phase margin which can make the system unstable in its response. Hence, it is essential that such a lag compensator is used which acts as a perfect PI (Proportional-Integrator) and has a pole nearly at the origin ( $0 \frac{rad}{sec}$ ), this way it will not reduce the phase margin to less than zero and would not make the system response unstable.

In Fig. 2.3 it can be observed that the compensator adds a very low-frequency high gain which results in the removal of steady-state error. In addition, the positive phase margin is also preserved which keeps the system from becoming unstable.

From Fig. 2.4 it can be observed that the compensator adds a very low-frequency high gain which results in the removal of steady-state error. In addition, the positive phase margin is also preserved which keeps the system from becoming unstable.

#### 2.4.1.2 Buck-Boost Converter

The system exhibits a persistent steady-state error, similar to the above-mentioned case of Buck Converter, mandating the incorporation of a low-frequency gain to amplify the initial response and subsequently address the persistent error. Therefore, we followed the same approach and used the applied control equation of the Buck converter. This also results in

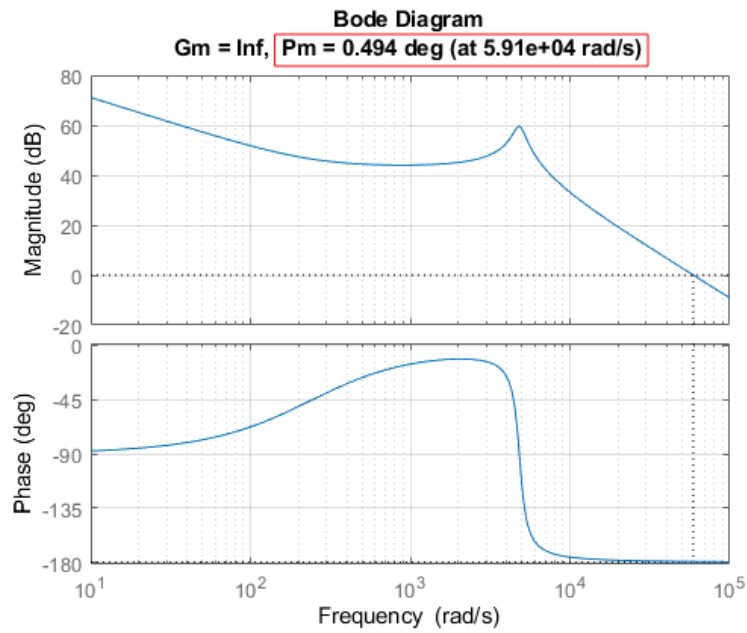


**Fig. 2.3:** Compensated Open-loop Frequency Response of Buck Converter

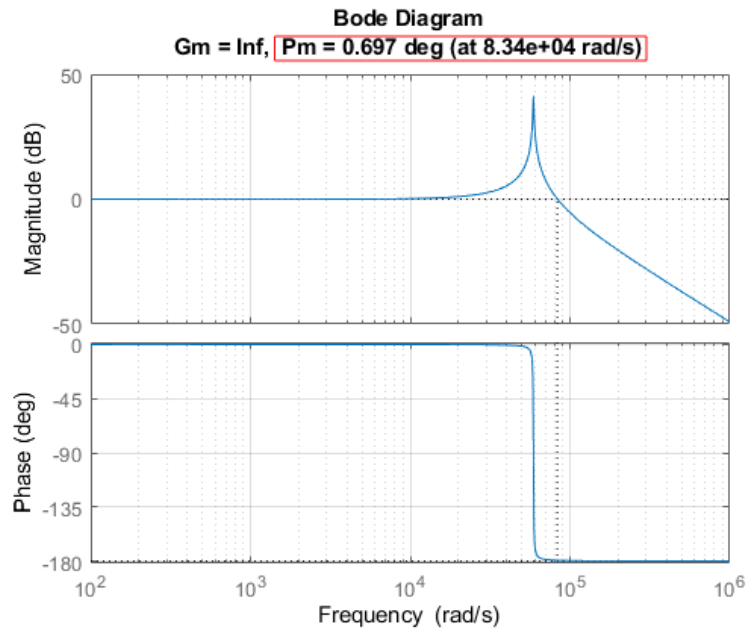


**Fig. 2.4:** Compensated Closed-Loop Frequency Response of Buck Converter

the elimination of steady-state error in the response of the Buck-Boost converter system. The system depicts a stable behavior on the application of the control equation, hence it can be said that the control equation suffices the regulator need of the system.

## 2.5 Programming and Testing

In both the Buck and Buck-Boost converter configurations, identical parameters are employed, and the same control equation governs their operation.

### 2.5.1 Application on Micro-controller

The control equation is operated and applied through the microcontroller. Due to this signals including PWM, and control input variations are also done throughout it. Therefore the control equation cannot be directly applied in frequency domain form. Hence it is converted into its time domain form where the integrator is represented as a cumulative sum of the error over fixed intervals of time (every 0.00002 seconds) which is then multiplied with the integral constant ( $K_i$ ). Whereas, the proportional part of the control equation is just the error multiplied with the proportional gain.

The control loop operates at a consistent sampling frequency of 50 KHz, implying that error computation and subsequent compensation occur on a per-cycle basis.

The selection of proportional-integral (PI) controller coefficients,  $K_i$  (integral gain) and  $K_p$  (proportional gain), is achieved through an empirical process, specifically the trial and error method. The chosen coefficient values have been determined as follows:  $K_i = 0.7$  and  $K_p = 1$ . These values represent the control gains that effectively regulate the converters' performance under the specified conditions.

#### 2.5.1.1 Control Parameters and Equation

Following are the equation and parameters that are applied on the converter systems for a compensated response.

$$G_c = K_p + \frac{K_i}{s} \quad (2.3)$$

Control Parameters	
Quantities	Value
$K_p$	1
$K_i$	0.7

---

## 3 SPI communication

---

For a fully optimized system, Precise temperature control of water inlet to inner heat exchanger and of test chamber are essential, and to achieve it, the power module which controls heater and cooler power rely on temperature sensors, the water flow rate and set temperatures. All the information necessary for temperature control is within the calorimeter mainboard. Thereby arising need for communication establishment between mainboard and power module. Power module gets the required data from the mainboard through Serial Peripheral Interface (SPI) communication. SPI communication is a widely adopted protocol in various applications, including embedded systems, digital electronics, and microcontroller-based setups. In this system SPI communication is implemented as shown in Fig.3.1, calorimeter mainboard referred to as master, the ADS1120 Analog-to-Digital Converter (ADC) referred to as slave-1 which is responsible for retrieving water temperature data from analog sensors and the calorimeter power module referred to as slave-2.

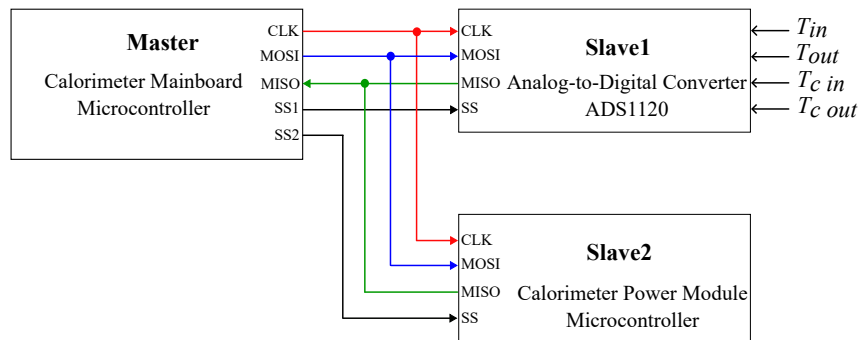


**Fig. 3.1:** Implemented SPI communication system

### 3.1 Protocol

The SPI communication happens between the master device (calorimeter mainboard microcontroller) and the two slave devices. After communicating with slave-1, the mainboard gets the digital values of the water temperature sensor analog data and processes, making it available for control purposes and sends the same to GUI. Subsequently, the master

proceeds to communicate with the calorimeter power module microcontroller, slave-2 for every one second.

The protocol for SPI slave-2, the calorimeter power module, involves the following steps. The master device sends inlet water temperature  $T_{in}$ , inner chamber temperature  $T_{test}$ , flow rate  $\dot{V}$ , and user-defined set temperatures for the inlet water and chamber, set via GUI. After receiving data from master, slave-2 transmits information regarding fault status, power consumed by both the cooler and heater to the master device through an interrupt service routine. This data from slave-2 is valuable for subsequent calculations related to power losses and overall system performance during testing and operation.

Upon receiving this required data, the temperature control loop within the calorimeter power module calculates and configures the necessary power settings for the cooler and heater. In addition to temperature data, the water flow rate is also an important parameter. Based on the flow rate, the cooler's temperature control parameters should be dynamically adjusted. This dynamic control ensures that the cooler maintains precise temperature, contributing to overall effectiveness in various operational scenarios.

## 3.2 Implementation and Testing

Commencing the debugging of the SPI communication code designed for slave-2 and its integration with the mainboard microcontroller pose an initial challenge, attributed to the complexity of the mainboard microcontroller code. To streamline the setup and simplify testing during SPI slave programming, a distinct master device was utilized. In the preliminary testing phase, the master microcontroller employed was of the same type as the one installed on the mainboard, and following successful code testing, it was integrated into the mainboard's code. Initially, instead of transmitting temperature and flow data, set power of the cooler and heater is transmitted from master. After receiving data, the slave-2 provides feedback by sending information about the actual power consumption of the heater and cooler. It also reports any issues related to data transfer and fault occurrences within the power module.

To ensure error-free communication, both the sender and receiver implement Cyclic Redundancy Check (CRC). CRC is a method of error checking that identifies errors in data during transmission. In the CRC process, the sender calculates the sum of all data bytes from the master before transmission. This sum value is then sent to the slave as the last byte. On the receiving end, the CRC program adds up all the received bytes, excluding the last one. By comparing this sum with the one received from the master, any transmission errors are detected. If the CRC program identifies errors in the transmission, it will discard the data and wait for the next data packet

Following testing with an alternate master, a successful SPI communication link was established between the master and Slave-2, enabling successful data exchange. Subsequently, proceeded to modify the calorimeter mainboard's code to transmit the necessary data to Slave-2.



---

## 4 Initial tests with heater and cooler - Milestone

---

After the successful implementation and testing of the inner voltage controller and SPI communication using an electronic load, the next testing phase involves applying real loads to the power module PCB within a calorimeter setup. This setup includes a resistive heater for the buck-boost converter and a peltier cooler for the buck converter.

The testing procedure was straightforward, the desired output power is set using the SPI master, and the power module adjusts the voltage to match the specified power. Throughout the testing process, the power module consistently performed well, maintaining stable power levels as required.

### 4.1 Observations

Below mentioned are some observations made during the initial testing with heater and cooler.

- Resistance correction: Initially, the impact of wire resistance is not taken into account and the resistance of both the heater and cooler is considered constant but varies due to their temperature coefficients. Later, the load resistance and wire resistance are calculated using real-time voltage and current measurement data.
- SPI communication interference: During SPI communication, encountered significant interference, causing the CRC program to discard the data sent by the master. This issue is resolved by placing ferrite noise filters at both ends of the SPI communication cable. These filters effectively captures and absorbs high-frequency electromagnetic noise generated by the cable or nearby sources.
- Furthermore, for safety reasons, over-voltage and over-current protection mechanisms has to be implemented for safeguard the heating and cooling systems from potential damage. This will be accomplished by using trip-zone submodule, and a detailed description is given in Chapter 5.

## 5 Trip-zone implementation

During testing, the MOSFETs and output capacitors were repeatedly damaged as a result of over-current and over-voltage conditions. To address these issues and safeguard the cooler and heater from over-current or over-voltage, protection measures are put in place using the enhanced pulse width modulator's (ePWM) trip-zone submodule.

The integration of the trip-zone submodule enhances system safety by closely monitoring voltage and current levels. If any of the voltage or current measurements exceed safe limits, the trip zone intervenes immediately stopping ePWM signals that control the converters and thereby protecting equipment from potential damage. Fig. 5.1 provides an overview of the implemented safety system. Using the analog pins depicted in Fig. 5.1, the microcontroller receives the measured voltages and currents. The microcontroller, utilized on the power module PCB, features all analog pins connection to the ADC module through an Analog Interconnect. Furthermore, the comparator is also linked to the same analog interconnect. If any of the analog values cross the safety limits defined within the comparator, the trip-zone submodule, connected through the multiplexer, promptly halts the ePWM gate signals to both converters. The outputs of the comparator are logically ORed before being transmitted to the ePWM module. The limits are set considering 1.25 times the voltage or current under full load conditions. Refer to [5] for detailed understanding.

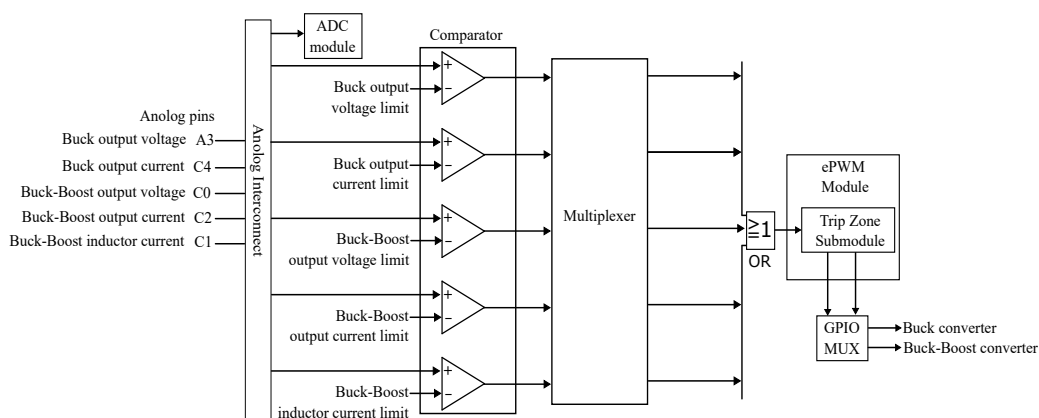


Fig. 5.1: Overview of trip-zone implementation

---

# 6 Power module PCB new version

---

The initial version of the power module PCB operates effectively, meeting essential criteria. Nonetheless, despite its satisfactory performance, the initial PCB version had some errors, necessitating modifications and improvements. Consequently, a redesign of the power module PCB is made to incorporate the needed corrections from the original version and to address new requirements.

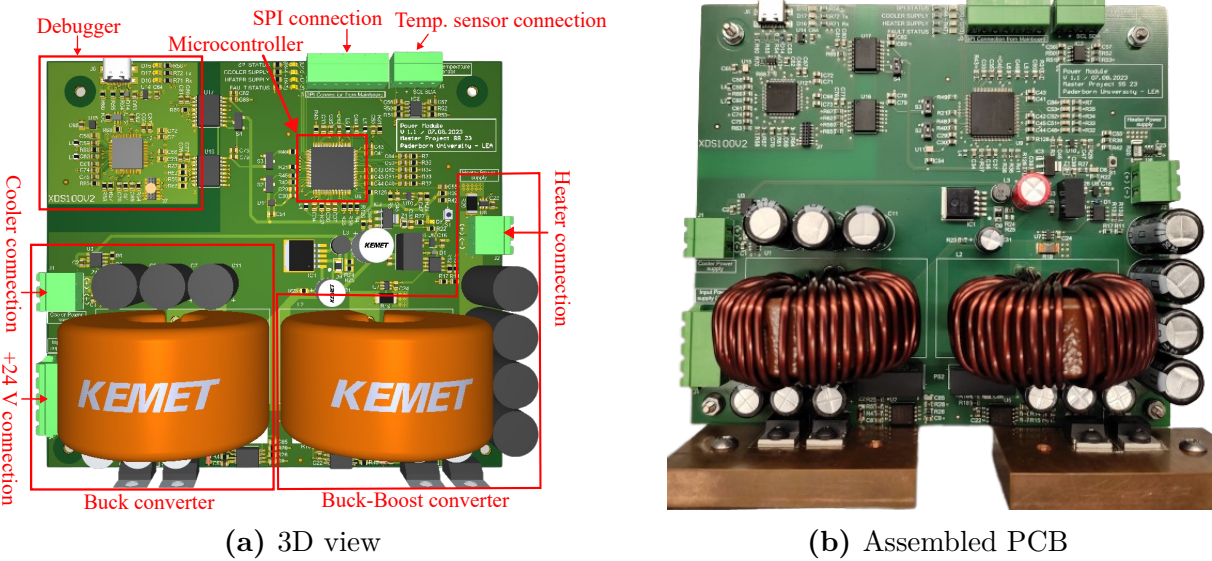


**Fig. 6.1:** Power module PCB version 1.1

Few important improvements made in the new version are:

- Careful selection of resistors and amplifiers for voltage and current measurement ensures the utilization of the entire 12-bit ADC range when the system operates at its maximum capacity. Moreover, high-precision 0.1 % tolerance resistors are employed in all measurement circuits.
- A temperature sensor has been integrated to monitor ambient temperature, facilitating automatic adjustments to the cooling system’s temperature settings. Once the

system is in fully functional for all operating points, the water inlet temperature  $T_{in}$  will automatically be configured to be 5 degrees lower than the ambient temperature.

- During experience with the previous version of the power module PCB, the output capacitors suffer damage due to their insufficient voltage and ripple current ratings. Consequently, they are replaced with capacitors that have higher ratings.
- To improve the over-current protection for the buck-boost converter, an inductor current measurement circuit is being introduced. This circuit aids in detecting high currents through the inductor when the MOSFET conducts.

## 6.1 Testing

The power module underwent complete in-house assembly. The Fig. 6.1b shows the fully assembled new version 1.1 of power module PCB that goes on to the calorimetric chamber. After assembling the second version of the PCB, the board testing phase begins. In the initial tests of the new board, no issues are detected. The ePWM and ADC signals are examined, and the converters are tested under varying loads, all functioning effectively. Both converters are tested up to 200 W of output power in open-loop with an electronic load. During testing, voltage, current, and power readings are recorded. The buck converter reaches 200 W at a 90 % duty cycle, while the buck-boost converter achieves this with a duty cycle below 60 %, using a load resistance similar to that of the heater and cooler. Accurate voltage and current measurements are crucial in the project, and the measurement circuits in use consistently gives precise results. A comparison between measurements obtained from these circuits and those acquired from highly calibrated digital multi-meters shows an very small discrepancy. Once voltage and current measurements become available, power calculations are performed and then matched with the power displayed on the electronic load. The percentage error between calculated power and the power measured by the electronic load is less than 0.5 %. Fig. 6.2 shows the percentage error of the Buck and Buck-Boost converter's output power.

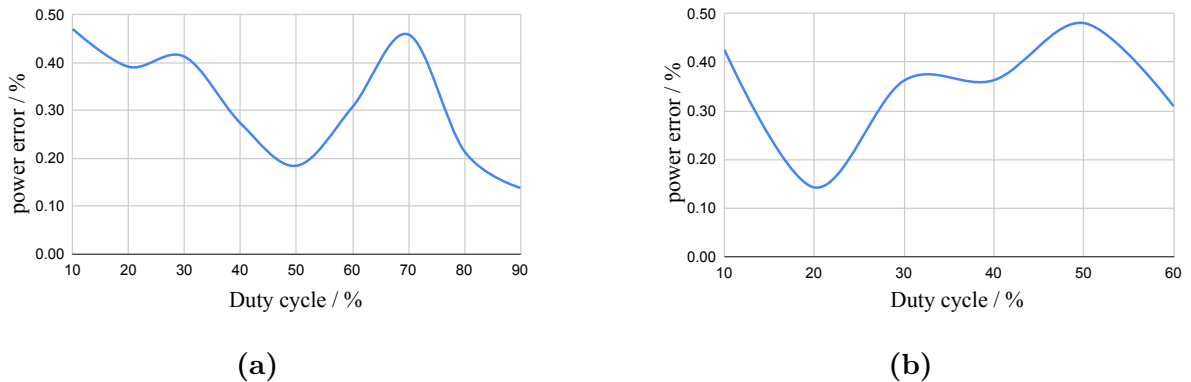


**Fig. 6.2:** (a) Buck converter's, (b) Buck-Boost converter's output power % error

---

# 7 GUI updates

---

## 7.1 Purpose

The control design framework implemented through the MATLAB Graphical User Interface (GUI) serves a dual purpose: first, it allows the user to specify target values for the cooling system and heater setpoint; second, it provides a means to visually analyze the system's response by presenting temperature-related data graphically. The graphical representation on the GUI encompasses the following temperature metrics:

- Water Inlet Temperature - Wasser Zulauf
- Water Outlet Temperature - Wasser Rücklauf
- Cooler Outlet Temperature - Temperature Cooler Outlet
- Inner Chamber Temperature - Lufttemperatur Hüllkammer
- Temperature of the Gap between the Inner Chamber and the Central Covering Chamber - Lufttemperatur Prüfkammer
- Cumulative Heat Loss, indicating power dissipation within the Inner Chamber for the Device Under Test (DUT) - Verlustleistung
- Water Volume Flow - Massenstrom
- Heater Set Value - Temperatur-Konditionierung
- Water Volume set value - Volumenstrom Pumpe

Furthermore, during system operation and measurement procedures, the ability to manipulate volume flows inside and outside the chamber is available.

## 7.2 Updates

Several updates were introduced to enhance the functionality of the GUI:

- Addition of a dedicated field to input set point values for the cooler - Kühler-Einstelltemperatur

- Power supply to the inner test chamber - Heizleistung
- Power supply to the Cooler - Kühlerleistung
- Real-time temperature display for the cooler outlet - Temperaturkühler-Auslass

The purpose of adding the above-mentioned fields and graphs is to allow user input for set values of heater temperature and cooler temperature to visualize the behavior of the system, analyze the power flow of the heater and cooler, and monitor the temperature of the water going into the chamber. By doing so, it becomes possible for the user to determine the performance of the overall chamber and to detect anomalies due to any malfunction that might occur. Following is the visualization of the updates made in the GUI.

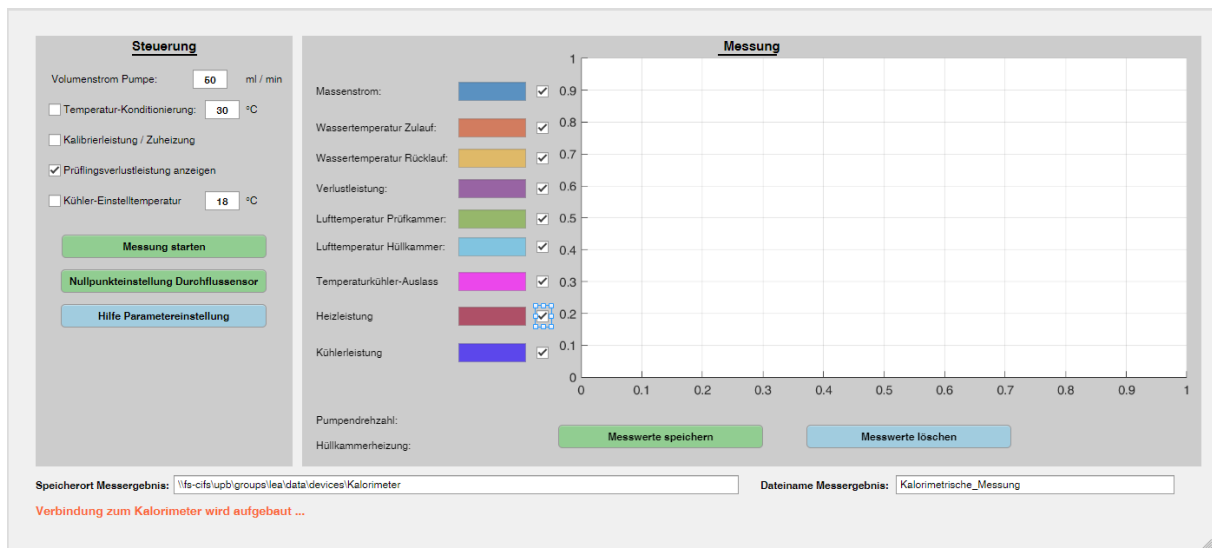


Fig. 7.1: MATLAB Updated GUI

Figure 7.2 is a closer frame of the GUI for a better view.

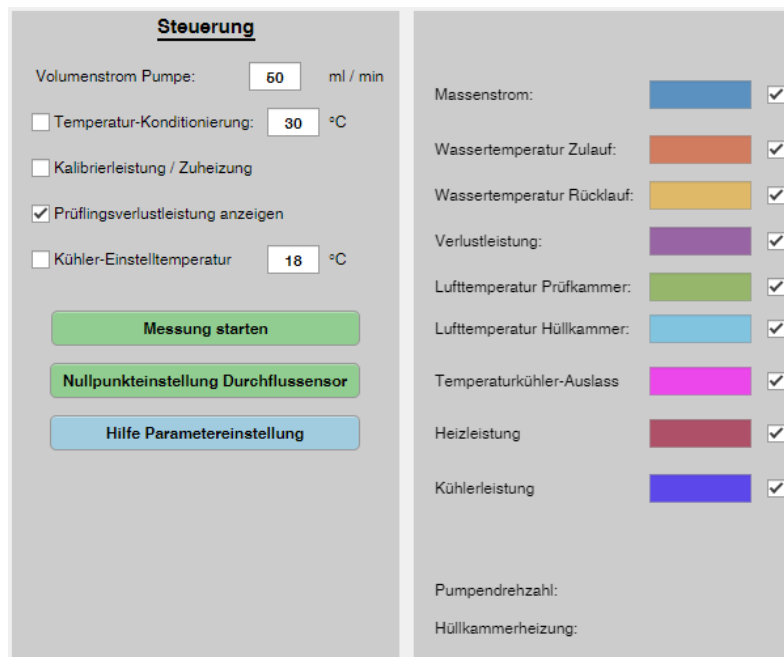


Fig. 7.2: GUI Data Fields and Graphs

### 7.3 Integration and Testing

Following the integration of these alterations within the GUI and subsequent synchronization with the main board code, the preset values are received at the main board. These values are then transmitted to the slave module within the calorimeter power system, in conjunction with both analog and digital sensor data. This coordinated process facilitates comprehensive control and monitoring of the system, ensuring its operational efficiency and performance optimization.

---

# 8 Cascaded control

---

## 8.1 Overview

In the context of control systems, a cascade control configuration entails the utilization of multiple controllers in a coordinated manner. In the domain of converter systems, cascaded control specifically involves the concurrent control of voltage and current. In this approach, the output of the first controller serves as the reference point or set-point for the second controller. However, in the particular system under examination, a distinctive configuration is employed where the set-point for the voltage control loops of both the Buck and Buck-Boost converters is determined by the output of an external temperature control loop.

Within this system, temperature values are obtained from sensors placed strategically throughout the setup. These temperature measurements serve as inputs to the temperature control subsystem, enabling the system to calculate the deviation from the desired temperature as specified in the graphical user interface (GUI) set-point. Subsequently, the output from the temperature control loops for the heater and cooler is interpreted as the prescribed power level, which is then translated into the designated output voltage for the inner voltage control loops governing the behavior of the converters.

This intricate control architecture ensures that the thermal aspects of the system are carefully managed to maintain the desired temperature, and this, in turn, guides the voltage control of the converters, guaranteeing the overall stability and performance of the system. The following is a depiction of the cascaded control loop of the system in a block diagram.

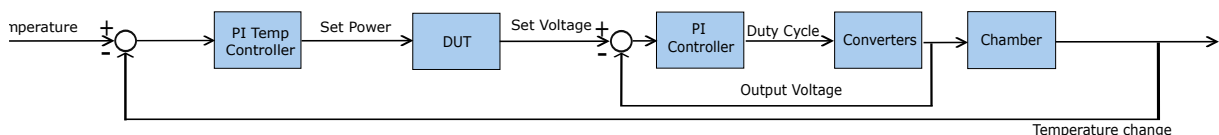


**Fig. 8.1:** Cascaded Control loop block diagram of System



Control Parameters		
Parameters	Cooler	Heater
$K_p$	1.80	22.9
$K_i$	0.120	0.013

**Tab. 8.1:** Temperature controller parameters for 100 ml/min flow rate

The temperature control in the above-cascaded control loop is implemented following the previous project [2]. However, for different set flow volume values, the parameters are different. The Tab. 8.1 gives PI parameters for a set flow rate of 100 ml/min.

---

## 9 Final tests and results

---

After testing everything implemented so far, calorimeter power module is mounted on the outer chamber as shown in Fig. 9.1.

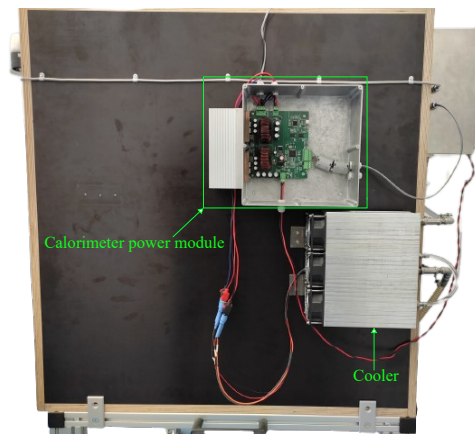
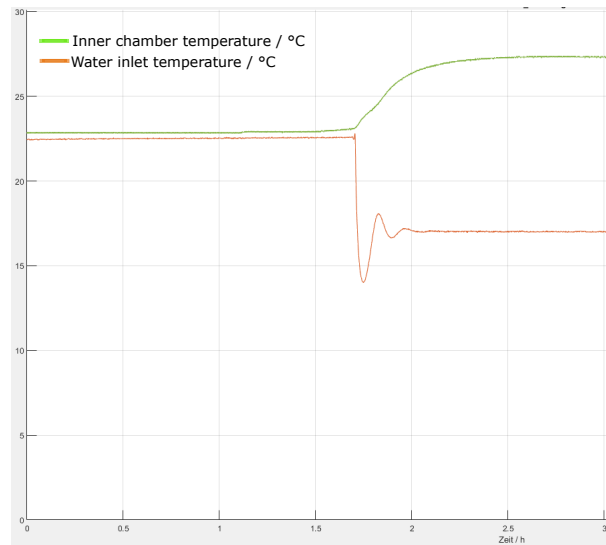


**Fig. 9.1:** power module integration

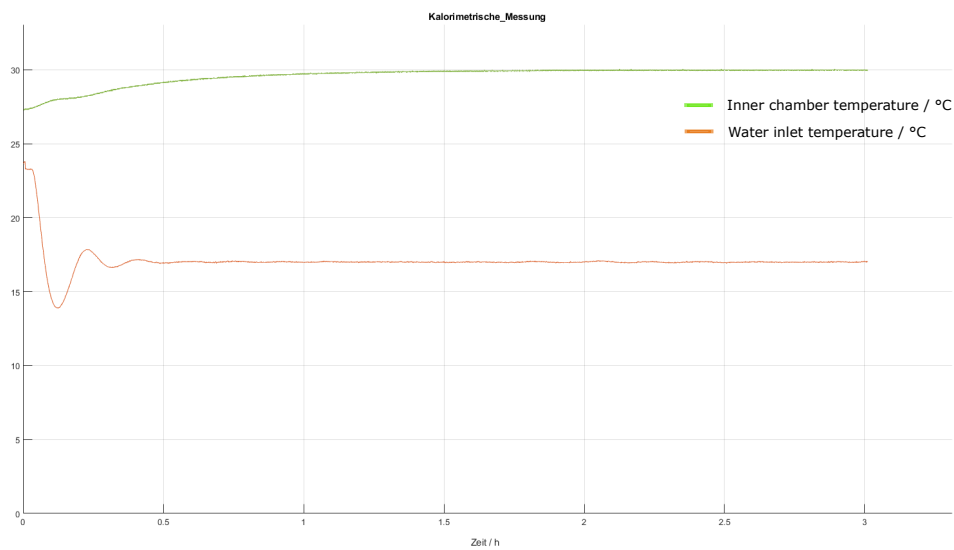
Fig. 9.2 depicts the conducted testing of the controllers at 17 °C for the water inlet temperature, with a 100 ml/min flow rate, and 27 °C for the inner chamber temperature. The implemented system achieves this target in under 1 hour. The Outer temperature controller parameters used are from Tab 8.1

Fig. 9.3 depicts the conducted testing of the controllers at 17 °C for the water inlet temperature, with a 50 ml/min flow rate, and 30 °C for the inner chamber temperature. The implemented system achieves this target in under 1 hour using PI parameters from Tab 9.1

Fig. 9.4 depicts the DUT loss measurements are performed using a 60 W resistive load placed in the test chamber and conducted testing of the controllers at 17 °C for the water inlet temperature, with a 100 ml/min flow rate, and 30 °C for the inner chamber temperature. The figure also shows the total losses of 90W along the heater and cooler consumed power. Calculated DUT loss using equation 1.2 is 61.7 W and the power analyzer



**Fig. 9.2:** Water Inlet and Inner Chamber Temperatures at set point 17 °C and 27 °C with 100 ml/min flow rate



**Fig. 9.3:** Water Inlet and Inner Chamber Temperatures at set point 17 °C and 30 °C with 50 ml/min flow rate

measurement reading is 60.05W. The implemented system achieves this target in under 1 hour and the calculated DUT loss accuracy is 97.2 %.

Control Parameters		
Parameters	Cooler	Heater
$K_p$	3.0	22.9
$K_i$	0.05	0.013

**Tab. 9.1:** Temperature controller parameters for 50 ml/min flow rate

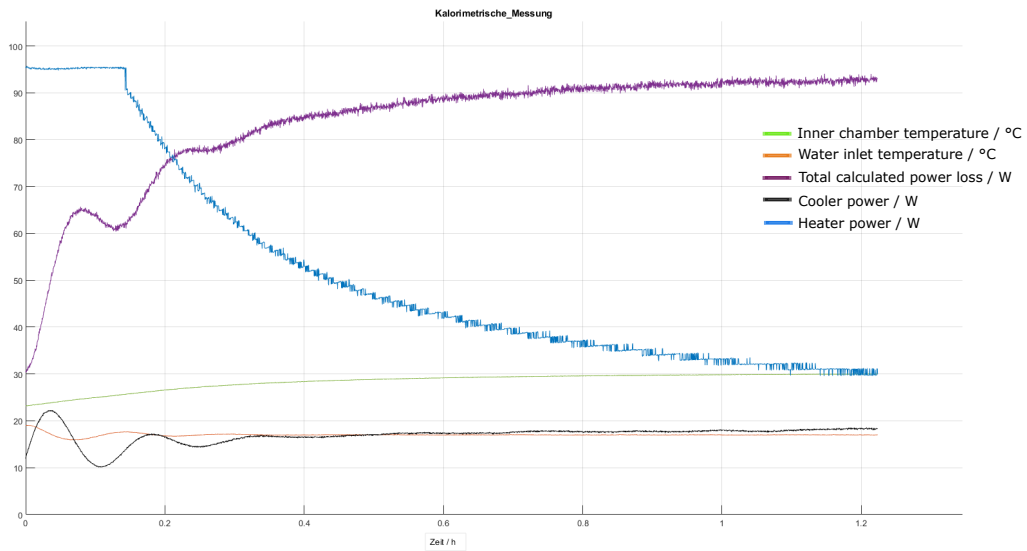


**Fig. 9.4:** 60 W DUT loss measurement

---

# 10 Conclusion and Future work

---

The project has successfully accomplished several key tasks. It began with the design and implementation of a cascaded control system, involving external temperature and internal voltage controllers, aimed at ensuring precise temperature regulation across all system components. Another crucial achievement is the implementation of the SPI communication protocol, enabling data exchange and coordination between the calorimeter mainboard and the power module. Furthermore, the power module underwent a redesign, incorporating necessary modifications and updates to enhance the optimal functionality. Lastly, comprehensive testing was conducted at multiple temperature points for water inlet and chamber temperatures, to validate the system's performance.

## 10.1 Future Work

Here are the aspects where enhancements can be made for future work:

- Refining the cooler control parameters to achieve the desired inlet water temperature for a predetermined flow rate, taking into account the expected DUT loss.
- Optimization of heater control parameters such that the set chamber temperature can be reached much quicker by slight adjustment of the outer temperature controller parameters.
- Incorporating an ambient temperature sensor into the power module PCB to enable the automatic adjustment of the water inlet temperature, maintaining it at 5 °C below the current ambient temperature without requiring manual input from the user.
- A minor update for the next version of the power module PCB: Presently, the cooler fans are continuously powered at +24 V, regardless of whether the cooler is operating or not. This can be improved by establishing a separate connection for the 24 V cooler fans, ensuring they only operate when the cooler is active.

---

# Appendix

---

## A.1 GUI

---

File name	description
Kalorimeter-BenutzerschnittstelleV8	Updated MATLAB GUI with field and set-point input changes

---

## A.2 CCS program

---

File name	description
Calorimeter Power Module	Implemented SPI program code. It also includes code implementation for Trip-zone along with control loops (Cascaded outer and inner control loops)
KalorimeterF280049C	Changes were made to integrate SPI communication with slave 2 and to incorporate updated GUI changes.

---

---

# Lists

---

## List of Tables

8.1	Temperature controller parameters for 100 ml/min flow rate . . . . .	21
9.1	Temperature controller parameters for 50 ml/min flow rate . . . . .	24

## List of Figures

1.1	Closed double-cased type calorimetric measuring chamber . . . . .	2
1.2	Schematic representation of optimized calorimetric measuring chamber . .	3
2.1	Inner Control Loop . . . . .	5
2.2	Uncompensated Frequency Response of Buck Converter . . . . .	8
2.3	Compensated Open-loop Frequency Response of Buck Converter . . . . .	9
2.4	Compensated Closed-Loop Frequency Response of Buck Converter . . . . .	9
3.1	Implemented SPI communication system . . . . .	11
5.1	Overview of trip-zone implementation . . . . .	14
6.1	Power module PCB version 1.1 . . . . .	15
6.2	(a) Buck converter's, (b) Buck-Boost converter's output power % error . .	16
7.1	MATLAB Updated GUI . . . . .	18
7.2	GUI Data Fields and Graphs . . . . .	19
8.1	Cascaded Control loop block diagram of System . . . . .	20
9.1	power module integration . . . . .	22
9.2	Water Inlet and Inner Chamber Temperatures at set point 17 °C and 27 °C with 100 ml/min flow rate . . . . .	23
9.3	Water Inlet and Inner Chamber Temperatures at set point 17 °C and 30 °C with 50 ml/min flow rate . . . . .	23
9.4	60 W DUT loss measurement . . . . .	24

## References

- [1] D. Christen, U. Badstuebner, J. Biela, and J. W. Kolar, “Calorimetric power loss measurement for highly efficient converters,” in *The 2010 International Power Electronics Conference - ECCE ASIA* -, 2010, pp. 1438–1445.
- [2] V. Nidhin and A. M. Khan, *Calorimeter measurement optimization*, 2022.
- [3] V. K. R. Thera and A. R. Ambat, *Calorimetric measuring chamber optimization - power module pcb*, 2023.
- [4] S. A. Naqvi S. Paishwa Zuhair S. Sarim, *Control and design of non-isolated and isolated dc-dc step down converters*, 2021.
- [5] *Tms320f28004x real-time microcontrollers technical reference manual*, 2022. [Online]. Available: <https://www.ti.com/lit/ug/sprui33f/sprui33f.pdf?ts=1680952737441>.